VIP *Very Important Paper*

Operational Validation of a Power Distribution Algorithm for a Modular Megawatt Battery Storage System

Lucas Koltermann,*[a, b, c] Kevin Jacqué,[a, b, c] Jan Figgener,[a, b, c] Sebastian Zurmühlen,[a, b, c] and Dirk Uwe Sauer[a, b, c, d]

Large-scale battery storage systems have become popular for various grid services in recent years. A worldwide market growth for battery storage has led to increased competition in several grid service markets. Modular large-scale battery storage systems require a safe, highly available, and intelligent energy management system (EMS) in order to be economically competitive. One component of this EMS is the control for distributing the power requests between individual battery units of the large-scale battery storage system. As the EMS is usually undisclosed intellectual property of the system manufacturers, there is only little information on real-world operation available. To contribute, we present a rule-based power distribution algorithm (SPDA) in this paper and validate it through field tests on a 6 MW/7.5 MWh system that is providing frequency containment reserve to the German power grid. The results show that especially when combining different battery technologies, the SPDA can exploit individual technological strengths. In this way, the state of charge of the batteries, energy throughput and power load of the batteries can be controlled to extend the lifetime. Moreover, the SPDA managed to shift nearly 80% of the energy throughput to one battery unit to protect less cyclic stable batteries and make use of the advantage of cyclic stable battery technologies, while fulfilling all grid service requirements. By shifting those large quantities of the energy throughput to more cyclic stable battery units, the large-scale battery storage system experienced in sum up to 45% less cyclic aging with the SPDA than with a symmetrical power distribution algorithm. Furthermore, the operational efficiency of a large-scale battery storage system can be significantly improved via additional software adaptations of the power distribution, depending on the system layout.

Introduction

In order to successfully accomplish the energy transition, various energy storage technologies will be needed in the future to ensure the energy supply and grid stability.[1] Battery storage is one option that is already in use and gaining more importance in the future. Currently, stationary battery energy storage systems (BESS) are used for the provision of frequency containment reserve (FCR), the fastest national frequency regulation market in Germany.[2,3] Besides FCR, other applications are also available and potentially economical for BESS.[4] On the one hand, front-of-meter applications like ancillary services, spot market trading, grid boosting, grid voltage regulation or island operation are areas for large-scale BESS.[5–8] On the other hand, behind-the-meter applications like peak shaving, increase of self-consumption or uninterruptible power supply are implemented with battery storage systems.[8,9] For large-scale BESS, ancillary services are currently mostly chosen.[3] Due to the batteries' fast response time, market applications with a requirement of a faster reaction time like enhanced frequency response in the UK market are also feasible.[10]

To enable this large variety of applications and quick development of large-scale BESS, the energy management system (EMS) of the BESS is a key factor. The EMS can be adjusted for the different applications and also enables to incorporate additional features and improvements of the BESS via continuous software development. For BESSs with multiple battery units, an essential part of the EMS is a power distribution algorithm (PDA) which decides when which battery unit has to charge or discharge. The PDA can thus control energy throughput, C-rate of the battery units and the state of charge and thus influences the aging and efficiency of a large-scale BESS. The economics of BESSs can consequently be

[a]   L. Koltermann, K. Jacqué, J. Figgener, S. Zurmühlen, Prof. Dr. D. U. Sauer
      Institute for Power Electronics and Electrical Drives (ISEA)
      RWTH Aachen University
      52074 Aachen (Germany)
      E-mail: lucas.koltermann@isea.rwth-aachen.de

[b]   L. Koltermann, K. Jacqué, J. Figgener, S. Zurmühlen, Prof. Dr. D. U. Sauer
      Institute for Power Generation and Storage Systems (PGS)
      E.ON ERC, RWTH Aachen University
      52074 Aachen (Germany)

[c]   L. Koltermann, K. Jacqué, J. Figgener, S. Zurmühlen, Prof. Dr. D. U. Sauer
      Jülich Aachen Research Alliance
      JARA-Energy
      52056 Aachen
      and
      52425 Jülich (Germany)

[d]   Prof. Dr. D. U. Sauer
      Forschungszentrum Jülich GmbH
      Institute of Energy and Climate Research Helmholtz-Institute Münster: Ionics in Energy Storage (IEK-12))
      52425 Jülich (Germany)

Batteries & Supercaps

Research Article
doi.org/10.1002/batt.202200414

**Chemistry
Europe**

European Chemical
Societies Publishing

improved in terms of durability and lifetime as well as minimizing energetic losses.

The influence of the EMS and PDA software creates a need for further research and development in this field.[8]

As the power distribution algorithm (PDA) is part of an energy management system (EMS), the section about energy management systems outlines those and their developments. After that, factors of battery aging are discussed in section "Battery aging", since the PDA is supposed to have a positive influence on this. Finally, in section "Large-scale BESS M5BAT", background information on the modular multi-megawatt medium voltage battery storage system (M5BAT) BESS is presented that is used during the presented PDA field test. Since the BESS continuously provides FCR in all tests, FCR will briefly explain in the following section about FCR.

Frequency containment reserve

To keep the European interconnected grid stable, there are several types of control reserve.[11] FCR is the control reserve with the highest response time requirements.[12,13] Since battery storage easily meets the response time requirements, they are particularly well suited for FCR.[13] In Germany the provision of FCR follows a characteristic power curve, which is a linear function of the frequency deviation, defined by the transmission system operators.[14] Within this curve degrees of freedom (DOF) like 20% overfullfillment or the use of the deadband are allowed.[12,14,15] In this study the DOFs are not used.

The target grid frequency in the European grid is 50 Hz. The deadband is ± 10 mHz around 50 Hz. Within this zone no action is required. For grid frequencies lower than 50 Hz the FCR provided has to supply the power to the grid or discharge the battery unit. Charging the battery unit or taking power from the grid has to be done at frequencies above 50 Hz. At 50.2 Hz 100% of the offered FCR power has to be taken prom the grid while at 49.8 Hz 100% of the offered FCR power has to be delivered to the grid.[12,14,15]

Energy management systems

All BESS consist of one or often more different battery units. Especially in modular and hybrid BESS with multiple battery technologies the usage leads to a more complex control.[6,7,16–20] Therefore, an EMS is required to ensure that all battery units operate reliably.[16,17,19] Within an EMS, a PDA controls reliability, efficiency, battery aging and battery load. PDAs undergo only little investigation as they are typically not disclosed by storage system operator in order to be competitive in the markets.

Nevertheless, theoretical work on optimizing a PDA has been performed with a focus on energy efficiency.[21] The work by Chol et al. showed benefits in efficiency for frequency regulation services for a BESS in Korea. They showed system wide benefits but no battery individual advantages.[22] Mühlbauer et al. investigated and tested power flow control strategies

and validated their model in lab-scale tests.[23,24] Moreover, they performed further optimization in simulations to their PDAs.[25] In addition, Schimpe et al. developed and tested a PDA in a field application.[26] The optimization they performed does only include the reduction of operational time of a second power unit. Next to those developments and evaluations large-scale field tests have not been shown and most developments focus on energy efficiency of the overall system. The potential advantages on operation and battery level are missing in the literature. The development and field testing of the EMS including the PDA address this gap. The developments are applied at the multi-technology BESS M5BAT, where they directly influence efficiency and reduce battery aging. The results of these investigations also provide the corresponding field results for other battery storage operators and EMS developers.

Battery aging

To increase the economic value of a BESS, the battery aging is the crucial part of this. Many different factors influence the battery aging and have already been investigated. For a BESS and the PDA, the aging factors should be taken into account.

Usually, the aging of batteries is divided into calendar and cycle aging. While calendar aging describes the aging that the battery has without operation, cycle aging refers to any kind of energy throughput.[27] showed in their work that the temperature is influential to calendar aging but the storage state of charge (SOC) is one main driver of battery aging. In further testing procedures on different battery technologies, they confirmed the aging factors of SOC and temperature but showed the technology specific aging intensity.[28] For lithium-ion battery, high SOCs lead to accelerated aging, while for lead-acid batteries low SOCs increase aging. However, high temperatures lead to higher aging rates for both technologies. For cyclic aging, the mean SOC and the Depth of Discharge (DOD) plays a major role.[29,30] After aging tests[31] implemented an aging model and summarized the main aging factors for calendar aging to temperature and battery voltage while storage or SOC while storage.

For cycle aging, they pointed out the mean SOC, the DOD, the current rate (c-rate) and thus the energy throughput.[31] High DODs, high c-rates, and a high energy throughput accelerate the aging for examined both for lithium-ion and lead-acid batteries.

Hence a PDA must take the major aging factors into account to gain improvements.

Large-scale BESS M5BAT

The PDA proposed in this paper is specific developed on the M5BAT BESS, on which earlier research has been undergone.[16–20,32,33] Like shown in previous reports,[18,19] the M5BAT BESS consists of ten battery units with individual

inverters, which are connected to 5 transformers. In Figure 1, the basic structure of M5BAT is visualized.

The ten battery units have different sizes in energy storage capacity and are designed for different lifetimes in terms of cycle stability and calendar lifetime. The technical descriptions of the batteries are presented in Table 1. The introduced acronyms and shortened acronyms will be used in the results chapter. The battery units consist of three lithium-ion technologies and two lead-acid technologies. The lithium-ion-technologies are lithium-manganese-oxide (LMO), lithium-iron-phosphate (LFP) and lithium-titanate-oxide (LTO). The two lead-acid technologies are lead-acid batteries with liquid electrolyte (OCSM) and sealed lead-acid batteries with gelled electrolyte (OPzV).

The parallel structure of all battery units and inverters give the M5BAT BESS an advantage in terms of availability while making the efficiency a challenging topic.[34] The inverter efficiency of M5BAT has already be investigated before.[33] The low efficiency of the inverters at low loads (lower than 10% of

the nominal load) led them to introduce a inverter threshold power and an inverter hysteresis power.[16,20,33] Figure 2 illustrates their findings and solution. The inverter threshold power is marked in green in Figure 2 and is set to approximately 10% of the inverter nominal power which corresponds to 70 kW at M5BAT. The inverter hysteresis power is marked in red in Figure 2 and is set to approximately 30% of the nominal power which corresponds to 190 kW. The losses decrease when less inverters are used with higher loads instead of more inverters with lower loads.

Only if the overall system target power is less than 70 kW, an inverter is still charged with power generation regardless of the losses, since this is contractually necessary for the fulfillment of FCR provision. In the case of a target power larger than 190 kW, several inverters can be used, provided that each inverter provides more than the inverter minimum power. If several inverters are used, the power is distributed in the respective stage according to a percentage weighting from the
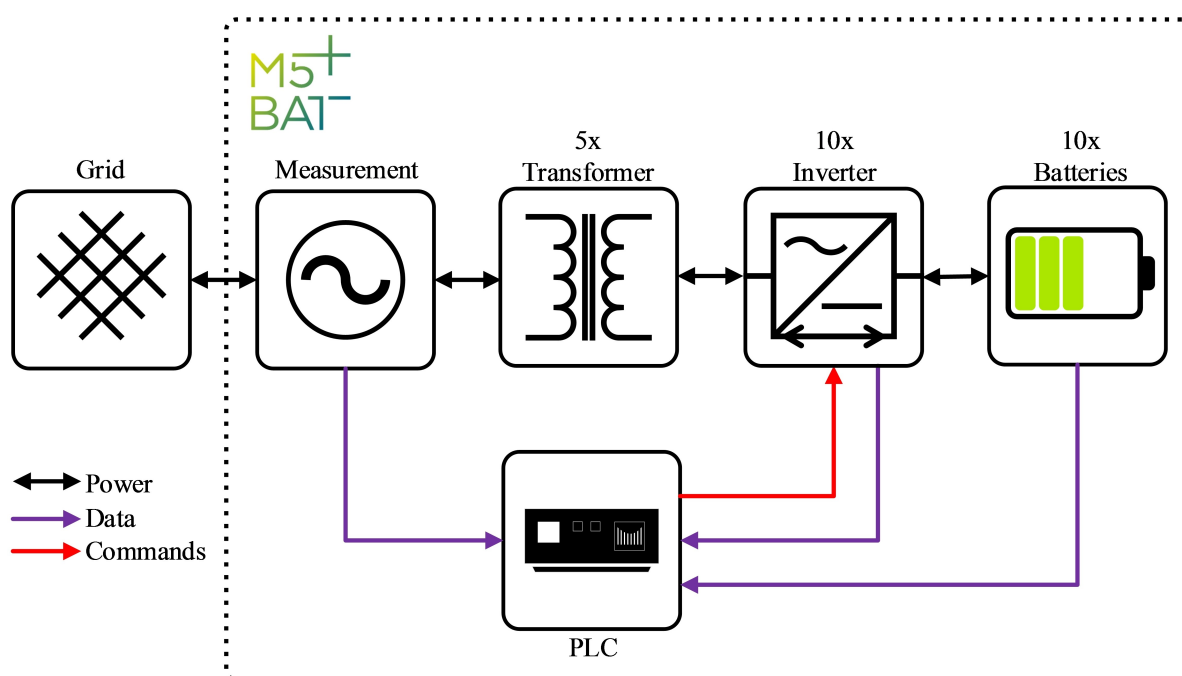

Figure 1. Basic structure of M5BAT own design according to previous research.[18,20]

Table 1. Technical battery description of the battery units and technologies of M5BAT.[19,20,32,34]

| Battery unit	Technology	Acronym	Short	Wiring	Voltage range per cell [V]	Nominal energy at 1/3 C [kWh]	Nominal capacity at 1/3 C [Ah]	Nominal number of cycles
1	OCSM	Pb1	P1	300s1p	1.7–2.4	1066	1776	1500
2	OCSM	Pb2	P2	300s1p (299s1p)	1.7–2.4	1066	1776	1500
3	OPzV	Pb3	P3	308s2p	1.7–2.4	843	1368	2400
4	OPzV	Pb4	P4	306s1p	1.7–2.35	740	1209	2400
5	LMO/NMC	LMO1	L1	192s16p	3.0–4.12	774	1088	6000
6	LMO/NMC	LMO2	L2	192s16p	3.0–4.12	774	1088	6000
7	LMO/NMC	LMO3	L3	192s16p	3.0–4.12	774	1088	6000
8	LMO/NMC	LMO4	L4	192s16p	3.0–4.12	774	1088	6000
9	LFP	LFP	L5	240s10p	2.8–3.45	923	1200	5000
10	LTO	LTO	–	312s32p	1.5–2.8	230	320	>12000
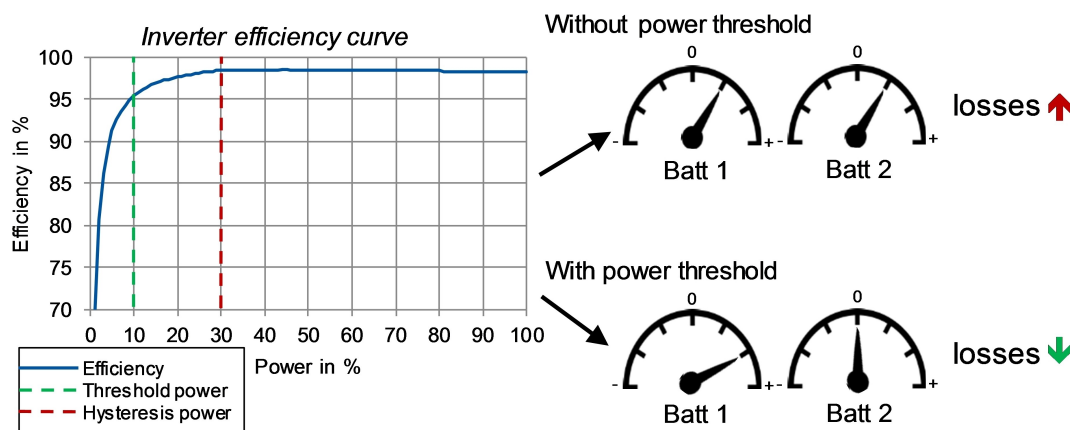
Figure 2. Left) Inverter efficiency curve; Right) effect of the use of an inverter power threshold on the losses at the inverters.[16,33]

sorting size, e.g., SOC or time to charge/discharge (see section "Modular staged-rule-based power distribution").[16,20,33]

In this work, we took the previous findings into account to develop and test a new modular-staged rule-based power distribution algorithm (SPDA). Thus, technology-specific advantages can be reasonably exploited in the operation of the BESS. As basic information for the calculation of the power distribution, the state of charge (SOC), the availability status (active, silent, stop) and power forecasts are transmitted from the battery management systems (BMS) of the individual battery units to the supervisory control and data acquisition (SCADA) system. As an input for the PDA, power forecasts of the battery units are made by the EMS. These power forecasts consist of power values (for each charging and discharging direction) the respective battery unit can provide for a certain time.

In the experimental section different PDAs are explained and a new SPDA is introduced. Moreover, some boundary conditions or additional algorithm parts are explained. The testing procedures and testing times are also discussed. Thereafter, in the results section, the overall test data is analyzed and the comparability is investigated. On the basis of five tests, the functionality of the new algorithm is demonstrated and the method of operation is shown and evaluated in Section "Evaluationof the power distribution algorithm".

Experimental Section: Power Distribution Algorithms

In the following, three power distribution algorithms and the testing procedures are presented. In addition to symmetric power distribution, the status quo PDA of M5BAT of the last years is presented for reference.

In order for a PDA to be activated, a target power value must be determined by the system. As can be seen in Figure 1, one single power value is required from the entire BESS. In the case of FCR service, the target power is set as a function of the grid frequency deviation. This power has to be provided by the BESS within 30 s in order to fulfill the FCR service. The PDA distributes the required power among the battery units. As shown in Figure 1, the target power calculation and the PDA runs on a programmable logic

controller (PLC). The PLC gives commands to the inverters which charge or discharge the battery units as requested.

Only active power is taken into account in the overall power distribution. The required reactive power is always distributed to the currently active unit. If no unit is active, the power is distributed to available units.

Symmetrical power distribution

The simplest form of a PDA is a symmetrical power distribution. In this case, the target power is divided equally among all available battery units. Here, the computational effort is minimal, but the efficiency of the system and technology-specific properties are not taken into account. Due to the low efficiency of inverters at low load, symmetrical power distribution is not ideal even for modular BESS with the same technology. A different algorithm should be chosen for the benefit of the battery units or the application.

Status quo power distribution

For a BESS to provide FCR, an algorithm to maximize the provisioning time is more appropriate than symmetric power distribution. In order to apply this algorithm, power forecasts for certain periods of time are required from each battery unit. The algorithm is thus dependent on the accuracy of the power forecasts. In Figure 3, a flowchart for the status quo algorithm is shown. Due to the sorting of the battery units by their power provision time the algorithm ensures that the BESS is as long as possible available for power requests. Thus, it is suitable for FCR providing assets, because according to the PQ condition, a minimum amount of energy and minimum power must be kept available for the delivery of FCR.[12] If a certain limit is reached, the SOC must be adjusted appropriately.[16]

For the M5BAT BESS the status quo algorithm was implemented according to Equation (1) and Figure 3. The available power forecasts for each battery unit for 60 min ($prognosis_{unit}(60min)$) and the instantaneous power forecast ($prognosis_{unit}(instant)$) were used.

$$t_{unit} = \frac{prognosis_{unit}(60min)}{prognosis_{unit}(instant)} \tag{1}$$

After the calculation of the power output time (t_{unit}) for each battery unit, the battery units are sorted according to the charging or discharging time with a hysteresis of 6 min. The hysteresis
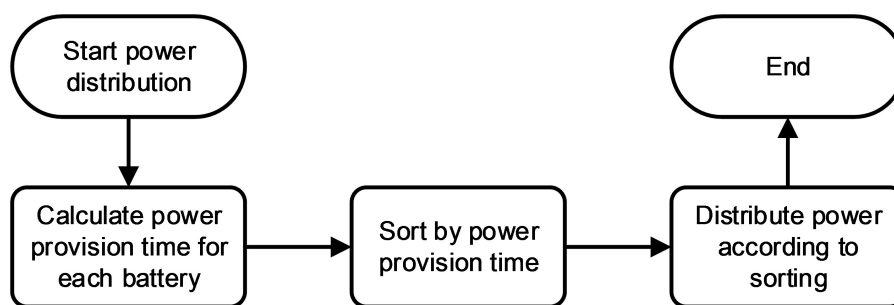
Batteries & Supercaps

Research Article
doi.org/10.1002/batt.202200414

Chemistry
Europe
European Chemical
Societies Publishing

Figure 3. Flowchart of the status quo power distribution algorithm.

prevents the system from switching between different battery units if they have nearly the same sorting value. The hysteresis value is adjustable. The sorting according to charging or discharging times is dependent on the power request.

The status quo power distribution algorithm and the output quality is thus reliant on the quality and availability of the power forecast values of each battery unit. In addition, the algorithm disproportionately favors battery units with a high energy to power ratio (EPR). A battery unit with a large energy content but low efficiency would take over a large share of the energy throughput.

To improve the named disadvantages the modular SPDA was developed and tested.

Modular staged-rule-based power distribution

To take advantage of different battery technologies, the operation of the different battery units must be adapted to the individual battery aging behavior, battery efficiency and availability (see[19,32,34] and "Evaluation of the power distribution algorithm"). The staged rule-based power distribution algorithm (SPDA) is designed to use the battery units in a way that power output, efficiency and aging are optimized and therefore the economic benefit of the battery storage increases.

The SPDA consists of four prioritization levels. In Table 2, the four levels of the algorithm are introduced with their boundary conditions, while in the following sections every level is explained individually.

Several SPDA levels can be activated separately and independently for each battery unit. Level 3 is always active by default, cannot be disabled, and serves as the last instance for all units. Power distribution always starts at level 1 and only a target power is passed to the next prioritization level if the previous prioritization level could not distribute all the power.

The flowchart in Figure 4 shows how each level of the SPDA is performed. Before all calculations are made, the boundaries from Table 2 are checked. Only if the boundaries are met the level of the SPDA is activated and otherwise the power request is passed on to the next level. If the boundaries are met, the sorting variables are calculated. The sorting variables are different for each level an

explained in the following sections. After sorting the battery units by the calculated sorting variables, the power is distributed. If the full power request could not be handled by this level, the remaining power request is hand over to the next level.

The individual levels are described in the following sections, but refer back to the state diagram in Figure 5. The diagram in Figure 5 shows for each level of the SPDA two exemplary battery units and two different states. State 1 is always the starting state and State 2 is the ending state. The change in between is only valid for a discharging process.

Level 1 (cyclic prioritization)

For prioritization level 1, a power limit and an SOC band must be defined for the battery units of this level (green areas in Figure 5). If the battery unit for which level 1 has been activated is in the predefined SOC band, the target power is distributed to this unit up to the power value set here, irrespective of the inverter hysteresis power. If prioritization level 1 is activated for several units, the power is distributed to these units up to the sum of the set power limits. If the units leave the set SOC band, this prioritization level is only used in one direction. If the units fall below the SOC band, it is only used in the charging direction, and if they exceed the SOC band, it is only used in the discharging direction. In Figure 5 for level 1 and state 1 two batteries are shown. The SOC of battery 1 is inside the level 1 SOC band while battery 2 is not activated for level 1 but instead for level 2. If battery 1 can fulfill the power request all options for other levels are not relevant. In the shown case in Figure 5 battery 1 gets discharged and battery 2 does not do anything. As long as the power requests can be fulfilled and the boundaries are met for battery 1, battery 2 is in a standby state.

Prioritization level 1 is suitable for cycle-stable battery units, since selected units will provide the most energy throughput for example when applying the frequency containment reserve. In addition, efficiency advantages like the mentioned hysteresis power of the inverters are not taken into account. Lithium-ion batteries like the LTO battery unit at M5BAT are well suited for this level. Due to the technical issues with the LTO battery unit the LMO battery units are tested for this prioritization level.

	Description	Boundaries
Table 2. Levels of the staged-rule-based power distribution algorithm.		
Level 1	Prioritization of a unit when a power threshold and SOC band are set.	Power P within a SOC band
Level 2a	Prioritization of a unit according to distance from the target SOC band	Predefined SOC band
Level 2b	Prioritization of a unit according to distance from the SOC boundary within a SOC band.	Predefined SOC band
Level 3	Prioritization of a unit according to predicted energy content	$E = prognosis(60\ min)$

Batteries & Supercaps

Research Article
doi.org/10.1002/batt.202200414

Chemistry Europe
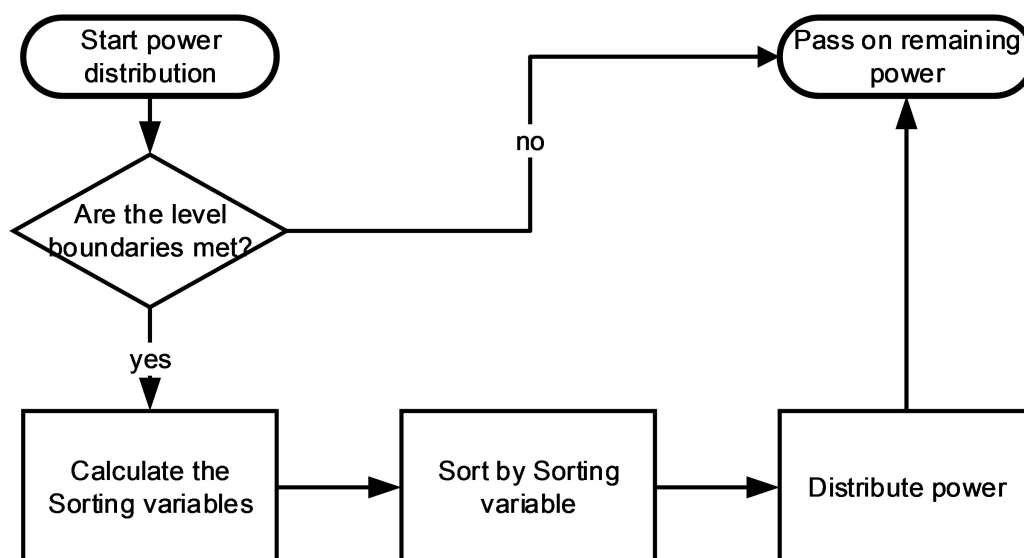European Chemical
Societies Publishing

Figure 4. Flowchart of the process of each level of the power distribution algorithm.
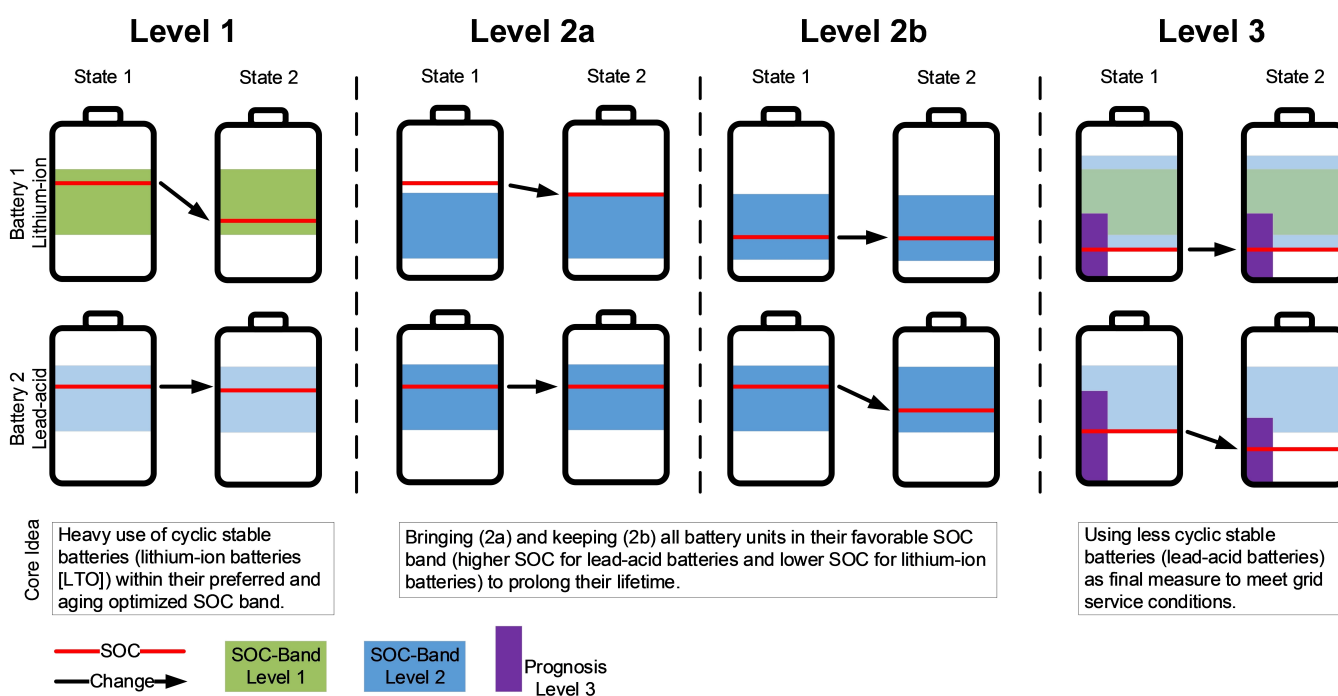

Figure 5. State diagram for each level of the power distribution algorithm (only discharging direction as example).

Level 2 a /2 b (SOC prioritization)

A common SOC band is defined for prioritization levels 2a and 2b. However, both stages can be activated separately. In level 2a, the distance to the specified SOC band is determined as a sorting variable. There is a hysteresis of the SOC of 5%. If the target SOC band of the unit is undercut, the unit can be charged; if the target SOC band is exceeded, the unit can be discharged. For level 2a both batteries in Figure 5 are activated. Battery 2 is already within the defined SOC band while battery 1 exceeds the SOC band. The discharging request will be fulfilled by battery 1 because battery 2 cannot be taken into account for level 2a because this battery does not meet the boundary conditions. Through the discharging

process both batteries in Figure 5 reached the SOC band in state 2 of level 2a.

Thus, the target SOC band can be "approached" with level 2a for each battery. If all units for which stage 2a is activated are within the target SOC band, prioritization level 2b takes effect. In level 2b, only units that are within the preferred SOC band are considered. Within the SOC band, the distances to the borders of the SOC band are calculated as a sorting variable. For the charging direction, the distance to the upper SOC boundary is determined and the units are sorted by distance with a hysteresis of 5%. For the discharging direction, the lower SOC limit is used analogously. In state 1 for level 2b in Figure 5 both batteries are within their individual SOC

Batteries & Supercaps

Research Article
doi.org/10.1002/batt.202200414

Chemistry
Europe
European Chemical
Societies Publishing

bands. The algorithm now calculates, that for battery 2 the range to the lower end of the SOC band is larger. Consequently, battery 2 gets discharged first. The hysteresis of 5% is chosen to prevent from toggling between multiple battery units if the distance to the boundaries is identical. The sorting algorithm holds the same output as long as those 5% are not crossed.

With the size of the SOC bands the energy throughput can be influenced. This means that larger SOC bands lead to larger energy throughputs. Based on this behavior the SOC bands for lithium-ion batteries are larger than for lead-acid batteries. Also, the SOC band for the lithium-ion batteries is generally lower than for the lead-acid batteries and exactly set to this in the BESS M5BAT.

If there is still power left to distribute after level 2a and 2b, the remaining power will pass on the next level of the algorithm.

Level 3 (energetic prioritization)

In prioritization level 3, which also serves as the "last instance" and is always active, the units are sorted according to available charging or discharging energy. The power forecast for 60 min ($prognosis(60\,min)$) is used as the energy and sorting variable. Units with the largest discharge power forecast are given priority for discharges and units with the largest charge power forecast are given priority for charges. Like shown in Figure 5 for level 3 both batteries undercut the boundaries for the previous levels. In that case only level 3 is active. For battery 2 the power prognosis is larger than for battery 1. Hence, battery 2 gets discharge at first. In state 2 both batteries have the same power forecast. As before in level 2a and 2b the sorting algorithm has an implemented hysteresis to prevent the system from toggling between multiple batteries.

The level quality is dependent on the accuracy of the power forecasts of the BMS of the battery units. This level of the algorithm is computational simple and distributes all remaining power requests, but does not consider any technology specific advantages. Only the energy capacity at full load of the corresponding inverter of a battery unit is decisive for the use of the battery unit. According to Table 1 this stage leads to a preference of the lead-acid battery units Pb1 and Pb2.

SOC based setpoint adjustment

Setpoint adjustments (SPA) are a form of energy or SOC management for BESS to sustain flexible operation both in charge and discharge direction. To deliver the grid service FCR, a certain amount of energy and the capability of fulfilling the offered reserve power is mandatory.[12,16] If the SOC or the power forecasts get too low a recharging request is made. Similarly, if the SOC is too high, a discharge request follows.[16] described this procedure for the BESS M5BAT. There, the setpoint adjustments are requested based on the 15 min and 30 min forecasts.[16] Since 15 min is the criterion for providing FCR, the forecasts between 15 and 30 min are interpolated and the 20 min is used as the SPA request. The calculated 20 min forecast is used because there is a delay time of 5 min to a full quarter-hour until a setpoint adjustment request is answered with a setpoint adjustment starting signal. This rule remains active as a basis to FCR provisioning in principle.

Newly to the procedure[16] showed is a SOC band independent of the power forecast that can be defined for the entire system.[16] As soon as the SOC band is exceeded or undershot, a setpoint adjustment is requested. The charging or discharging power can be defined in advance. In an emergency when the set FCR power band is larger than the maximum available power forecast, the band is

also held disregarding the power difference so that a total outage of the battery storage is prevented. Currently the SOC band for the battery storage M5BAT is set to 35% to 70% SOC (SPA-SOC).

Power limitation

To protect certain battery units from excessive power and currents, the power predictions are limited to the maximum value according to Table 3. If no power limit is set for the batteries, the inverter defines the power limit, which is then set to 630 kW per battery unit.

The power limitation is for optional use and does only affect the PDA, when the prognosis for 60 min is higher than the set power limit. The necessity for a power limitation came from operation experience and helped to increase the availability of battery units with poor BMS implementations.

Testing procedure and testing times

To test the different levels of the presented SPDA five testing sessions were performed. In order to quantify and evaluate the different PDAs and settings, their effectiveness and differences, the following criteria for the evaluation are defined:

1. SOC distributions for the tests
2. Actual power delivered per battery unit
3. Energy throughput per battery unit
4. Overall system efficiency

All results are shown in the section "Evaluation of the power distribution algorithm".

In the following, the chosen options for the tests and batteries are shown. For all tests, the following requirements were fulfilled:

- 3 MW FCR
- SPA-SOC: 35–70%
- Seven following days per test without any outages or failures

The chosen options are shown in detail in Table 4. Tests 3 and 5 differ in the chosen battery unit for the level 1 prioritization. Also, the effect between only the level 1 and the combination of level 1 and 2 can be separated. Test 4 shows extreme settings of the level 2 prioritization for the battery units 5 to 8. This is to be able to examine the function in the event of an incorrect setting and its effects. Test 1 shows an energetic order that could be used as a standard for the maximum operating time. Test 2 shows only level 2 and 3 prioritizations. Here, aging minimizing SOC bands were selected.[28]

The chosen SOC bands in all tests support the core ideas of Figure 5 and the expected advantages described in the section

Table 3. Absolute power limitations for the battery units, valid for charging and discharging.

Battery unit	Power limit [kW]	Max. inverter power [kW]
Pb1	450	630
Pb2	450	630
Pb3	315	630
Pb4	315	630
LMO1	–	630
LMO2	–	630
LMO3	–	630
LMO4	–	630
LFP	–	630
LTO	–	630

Table 4. Options of the levels of the prioritization for the different tests.

Test	Battery unit ► / Level of prioritization ▼	1	2	3	4	5	6	7	8	9
0	status quo	Not performed for this evaluation. See evaluation done by previous work.[19,32,34]								
1	Level 1	For all battery units off								
	Level 2a,b	For all battery units off								
2	Level 1	For all battery units off								
	Level 2a,b	45%–70%				25%–60%				35%–70%
3	Level 1	off							40%–60%	off
	Level 2a,b	45%–70%				25%–60%				35%–70%
4	Level 1	For all battery units off								
	Level 2a,b	45%–70%				0%–60%				35%–70%
5	Level 1	off				40%–60% 300 kW	off			
	Level 2a,b	45%–70%				off		25%–60%		35%–70%
1–5	Level 3	For all battery units in every test on								

about the "modular staged-rule-based power distribution". The chosen SOC band for the lead-acid batteries starts 20% higher than for the lithium-ion batteries. The only exceptions were made to test out prioritization level 1. For this level SOC bands around 50% SOC were chosen.

Results and Discussion

The results of the investigation of the newly developed SPDA are divided into the general information including the comparability of the tests and the evaluation of the battery statuses. Afterwards the shown results are discussed and compared to the status quo PDA and a symmetrical PDA.

General information about the tests

In this section, the differences and similarities of the grid frequency in the different tests are highlighted. At first the frequency distributions are evaluated and then used to create a metric of the test comparability.

Frequency distribution

To best examine the settings of the SPDA, the tests are designed as similar as possible. Since part of the test is the continuous provision of FCR, the tests are dependent on the power grid status. Therefore, the frequency distributions per test are examined in the following.

Figure 6 shows the frequency distributions for each test as boxplots. The colored lines above or underneath the whiskers are outliers, when the frequency deviation is higher or lower for only a short period of time. The colored lines within the boxes (50% of all values) are the median values.

It can be seen from the boxplots that for all tests the frequency is between 50.05 Hz and 49.95 Hz. Among the outliers present, test 4 stands out, where single upward outliers are less pronounced than in the other tests. In contrast, the downward outliers are somewhat more pronounced in test 2 and test 4 than in the other tests. In tests 2 and 3, the frequency average is shifted slightly above 50 Hz. However, the outliers are only single values and account for a maximum of 0.7% of the data. Therefore, the conditions can be seen as quite similar for a field test.

Comparability of the tests

In order to evaluate and compare the evaluated results later, the parameter of the grid frequency of the different datasets are compared with each other in advance.

For each test the measured grid frequency is not exactly the same which would be ideal for a comparison. Table 5 shows a percentage number of the identical data points within the datasets. Each test is compared with each other test. As a result, more than 90% of the data points are equal.

As an error metric the mean absolute percentage error (MAPE) is chosen to show the comparability of the frequency datasets and consequently the required power output of the BESS. The error is calculated against 50 Hz which means any deviation from the target grid frequency is directly an error.

Table 5. Percentage of identical grid frequency data points in the datasets.

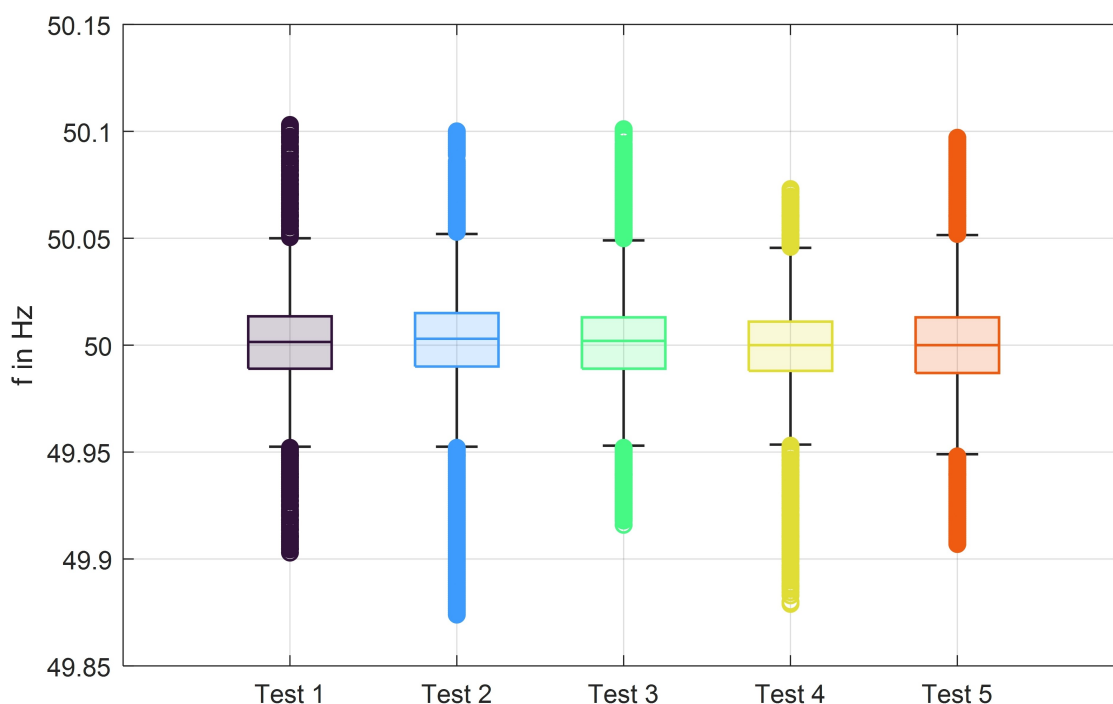| similarity,1	Test 1	Test 2	Test 3	Test 4	Test 5
Test 1	–	96.19%	96.89%	94.68%	96.82%
Test 2	96.19%	–	94.98%	91.75%	93.59%
Test 3	96.89%	94.98%	–	95.47%	94.71%
Test 4	94.68%	91.75%	95.47%	–	94.14%
Test 5	96.82%	93.59%	94.71%	94.14%	–

Figure 6. Distribution of the frequency for each test.

Equation (2) shows the used formula, while n is the number of data points, i is the current data point and f is the measured grid frequency. After calculating the errors, the difference of the errors between the complete dataset and the dataset for each test is calculated [see Equation (3)]. This key size is used to rate the similarity or difference of the test-datasets.

$$MAPE = \frac{100}{n} \sum_{1}^{n} \frac{f(i) - 50}{f(i)} \qquad (2)$$

$$Diff - MAPE = abs(MAPE_{all-datasets} - MAPE_{datasetX}) \qquad (3)$$

The results of the Difference-MAPE are listed in Table 6. The difference oscillates between 0.03 and 0.27. The calculated numbers can used as a percentage error on the following results.

Next to the Difference-MAPE, the distribution functions are shown in Figure 7. The distribution functions shape and expansion look very similar.

As a conclusion, the test data can be compared to each other despite the shown small differences in the datasets.

Evaluation of the power distribution algorithm

As described in section "Testing procedure and testing times" the testing results are limited to the SOC, power distribution, energy throughput and efficiency. For the SOC and power distribution only the results of test 6 are shown graphically, while all other test results can be found in the appendix.

SOC distribution

The SOC distribution for each test indicates whether level 2 of the SPDA is working as intended. The set SOC bands should be reached and maintained by all battery units.

Figure 8 shows the SOC distributions for all tests as boxplots. To increase the readability outliers are not shown as they only account for less than 0.7% of all values. The target dot within the boxplots marks the median value, while the red lines mark the upper and lower SOC bands for each battery and test.

Lead-acid batteries: Without using level 2 like shown in Figure 8 the SOC level of the lead acid batteries Pb1 and Pb2 is at a low status around 30%. Their large energy capacity and high discharge prognosis but low charge prognosis caused their general low SOC in test 1. For batteries Pb3 and Pb4 only the target point is visible which means that the batteries were not used and maintained the same SOC for the entire time. In all other tests the SOC bands for level 2a and 2b were set for the lead-acid batteries. With only a few exceptions those SOC bands were kept for all tests. The median value is always within the SOC band which was chosen at a higher level due to improved aging behavior for lead-acid batteries. For test 3 and
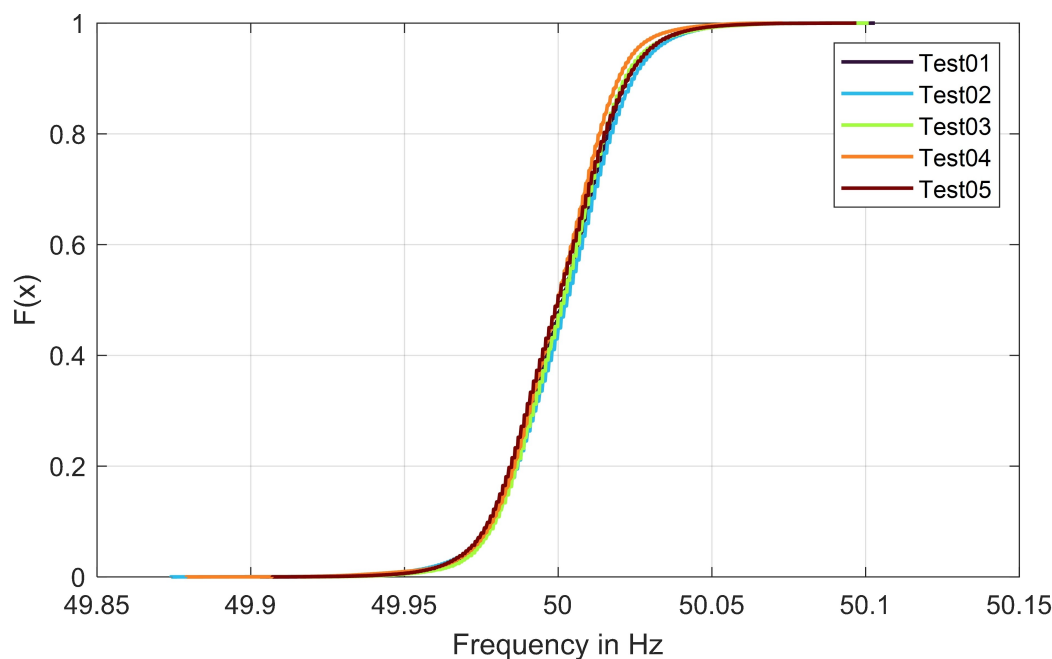
Table 6. Diff-MAPE according to Equation (3).				
Test 1	Test 2	Test 3	Test 4	Test 5
0.029	0.03	0.028	0.027	0.029

Figure 7. Distribution function of the measured grid frequency for each test dataset versus the sum of all datasets
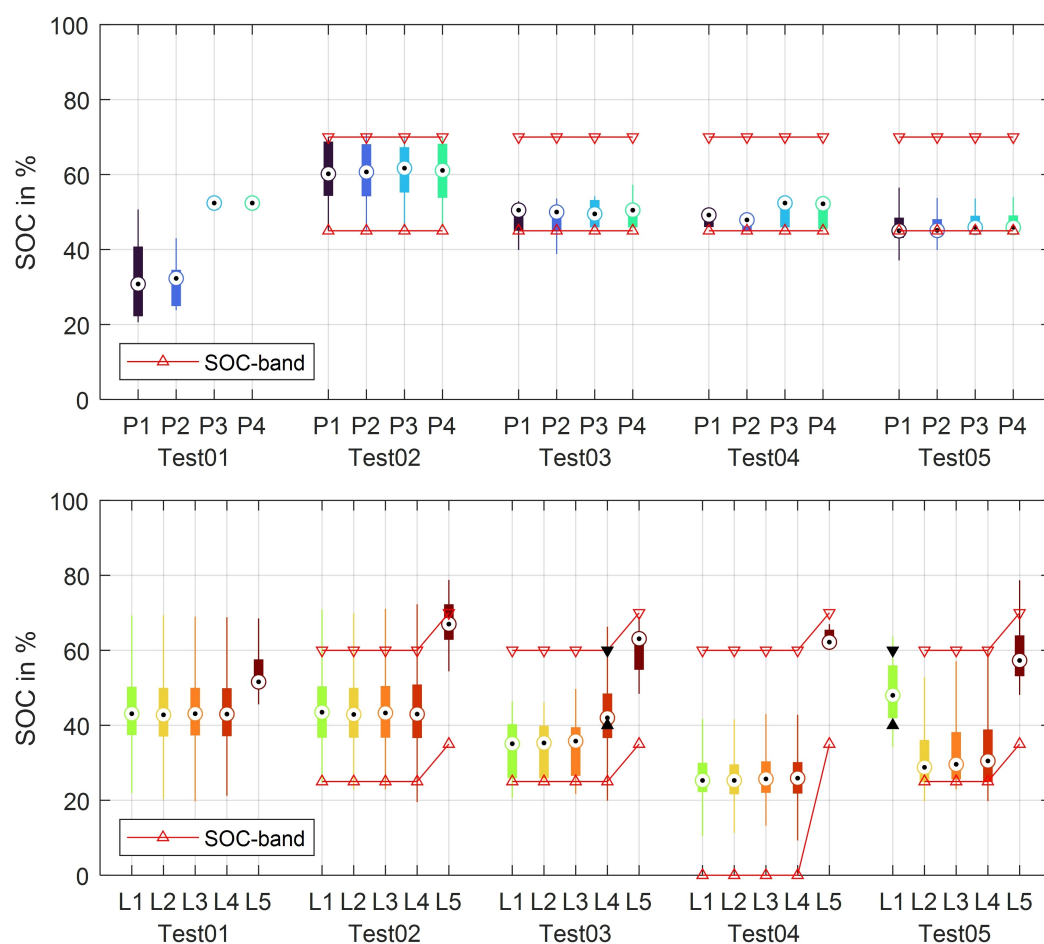

Figure 8. Boxplots of the SOC distribution for each battery unit of M5BAT. The upper subplot shows the lead-acid batteries while the lower subplot shows the lithium-ion batteries with the shortened acronyms according to Table 1. The red lines indicate the set SOC bands for level 2 according to Table 4, while black filled markers refer to the SOC band from level 1.[35]

5 the lower SOC boundary is undercut a couple of times within the test while this did not happen for test 2 and 4. The reason for undercutting the boundary is that only the battery unit active for level 1 has a higher SOC and all other batteries were in standby mode at the lower boundary. Higher power requests which could not be fulfilled by the battery unit in level 1 was automatically transferred to level 3 due to lacking discharging capabilities in level 2. In level 3 the lead-acid batteries had the higher discharge capabilities and were thus preferred.

Lithium-ion batteries: For the Lithium batteries SOC bands for level 2a and 2b are highlighted with red markers in Figure 8 while SOC bands for level 1 are marked with black filled markers. The SOC bands for level 1 are only used for battery L4 in test 3 and battery L1 in test 5. Starting with test 1 all lithium batteries are at medium SOC levels between 40% and 50% SOC. Due to different power prognosis and technologies battery L5 has an overall higher SOC. For test 1 to test 5 the SOC bands were used and for all lithium batteries the median SOC as well as most of the boxplots can be found within the targeted SOC bands. For using level 1 in combination with level 2 like in test 3 for battery L4 the SOC band from level 1 cannot be kept for the entire time. But if level 1 is used independent like in test 5 for battery L1 the targeted SOC band

is kept for nearly the entire time. Comparing test 4 to test 2 and test 1 it can be seen that through the SOC bands an overall lower mean SOC can be maintained compared to non-using the SPDA.

Regarding to the calendar aging behavior of batteries the presented level 2a and 2b of the SPDA is capable of reaching and keeping user set SOC ranges. For correct use of this level, the calendar aging of batteries can be lowered over a longer period of time.[28]

Power distribution and C-rate

The power distribution and C-rates are used to determine the functionality of level 1 of the SPDA.

In Figure 9 the power distribution for all batteries and tests are presented. Data points with a power value of 0 kW are not shown in this figure but can be found in the appendix. The boxplots for batteries P3 and P4 in test 1 are missing because those batteries hat no power output for the entire test.

For all batteries and all tests, the boxplots are within the 200 kW range while the whiskers reach up to 450 kW for battery P1 and P2, up to 315 kW for batteries P3 and P4 and up
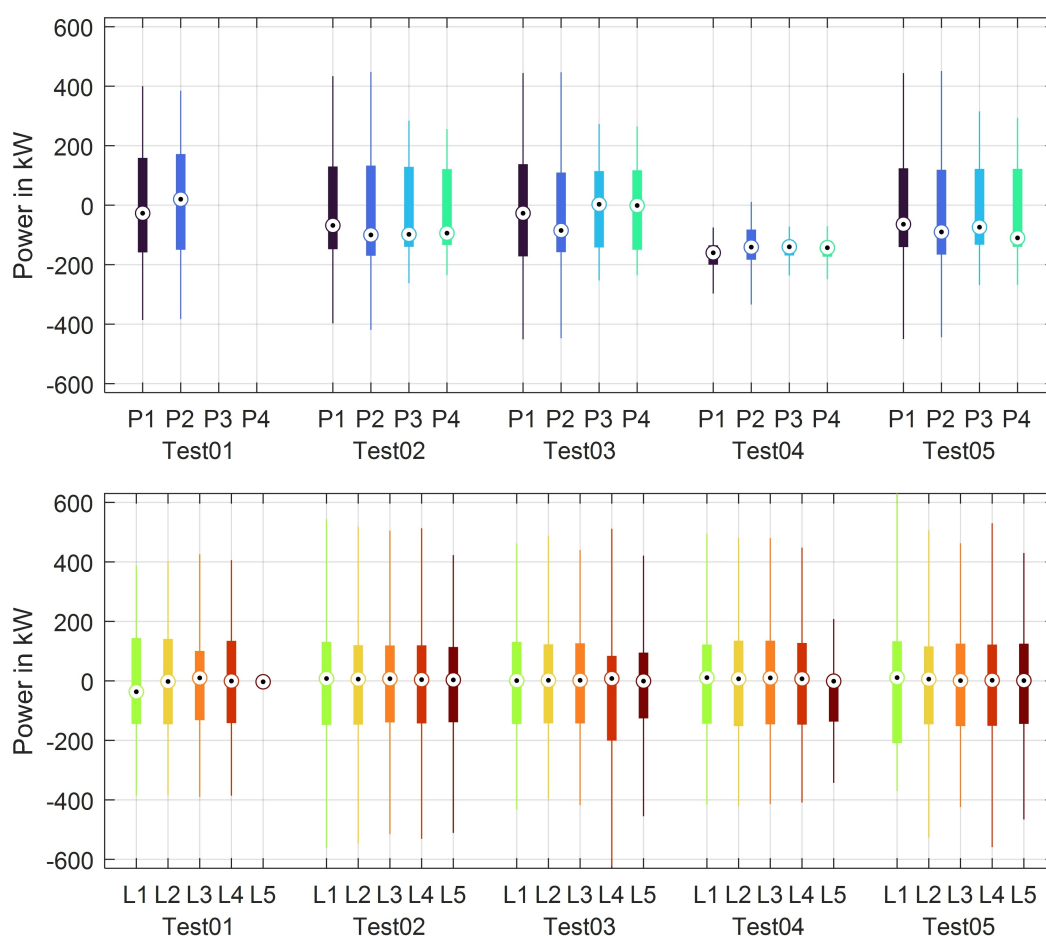
Figure 9. Boxplots of the power distribution for each battery unit of M5BAT. The upper subplot shows the lead-acid batteries while the lower subplot shows the Lithium batteries with the shortened acronyms according to Table 1. Data points with no power requests are not shown here but can be found in Figure A1 in Supporting Information.[35]

Batteries & Supercaps

Research Article
doi.org/10.1002/batt.202200414

**Chemistry
Europe**
European Chemical
Societies Publishing

to 500 kW for the Lithium batteries. Batteries L4 in test 3 and L1 in test 5 show higher whiskers up to 630 kW. Those batteries were used for level 1 of the SPDA and had thus more intense power requests.

The median value for the lithium-ion batteries is always nearly 0 kW while the median value for lead-acid batteries lies mostly below 0 kW. Due to a lower round-trip-efficiency (RTE) of the lead-acid batteries, those are charged more often to keep the SOC range. In test 4, the complete boxplots of the lead-acid batteries are in the negative power range. In this test, the lead-acid batteries are used very seldom and were nearly only charged which in sum does not add up to one equivalent full cycle.

To put the power distribution into a battery context, the C-rates are analyzed and illustrated in Figure 10. As before data points with a C-rate of 0 C are not shown, but can be found in Figure A2. Boxplots for batteries P3 and P4 in test 1 are missing because those batteries have not experienced any charge or discharge during the test.

Lead-acid batteries: The box of the Boxplots for the lead-acid batteries in Figure 10 covers C-Rates between -0.2 C and 0.2 C while the whiskers stretch out up to -0.3 C and 0.5 C. The median value is always negative with the exception of battery

P2 in test 1. This indicates that the battery was discharged more than charged and thus has a lower SOC after the test than before. The non-existing boxes in test 4 indicate again that the lead-acid batteries were only used rarely in this testing procedure.

Lithium-ion batteries: For the lithium-ion batteries, the C-rates are overall higher than the observed C-rates for the lead-acid batteries and reach up to ± 0.9 C. The boxplots for batteries L1 to L4 look similar to each other while battery L5 hast mostly lower loads than the other lithium batteries. Battery L5 is according to Table 1 a different technology from the other lithium batteries and has a higher energy capacity. While the inverter is still the same and the power requests are comparable the difference in energy capacity lead to lower c-rates for Battery L5. A higher load and thus larger boxes of the boxplots are observable for battery L4 in test 3 and battery L1 in test 5. Those are again the battery units for which level 1 of the SPDA was activated.

In Figure 10, the median value for all battery units (exception P2 in test 1) is negative. This shift is reasoned in the losses of the inverter and battery which results in more charging procedures than discharging. On the other hand, in Figure A2, all median values are 0 C because most of the time
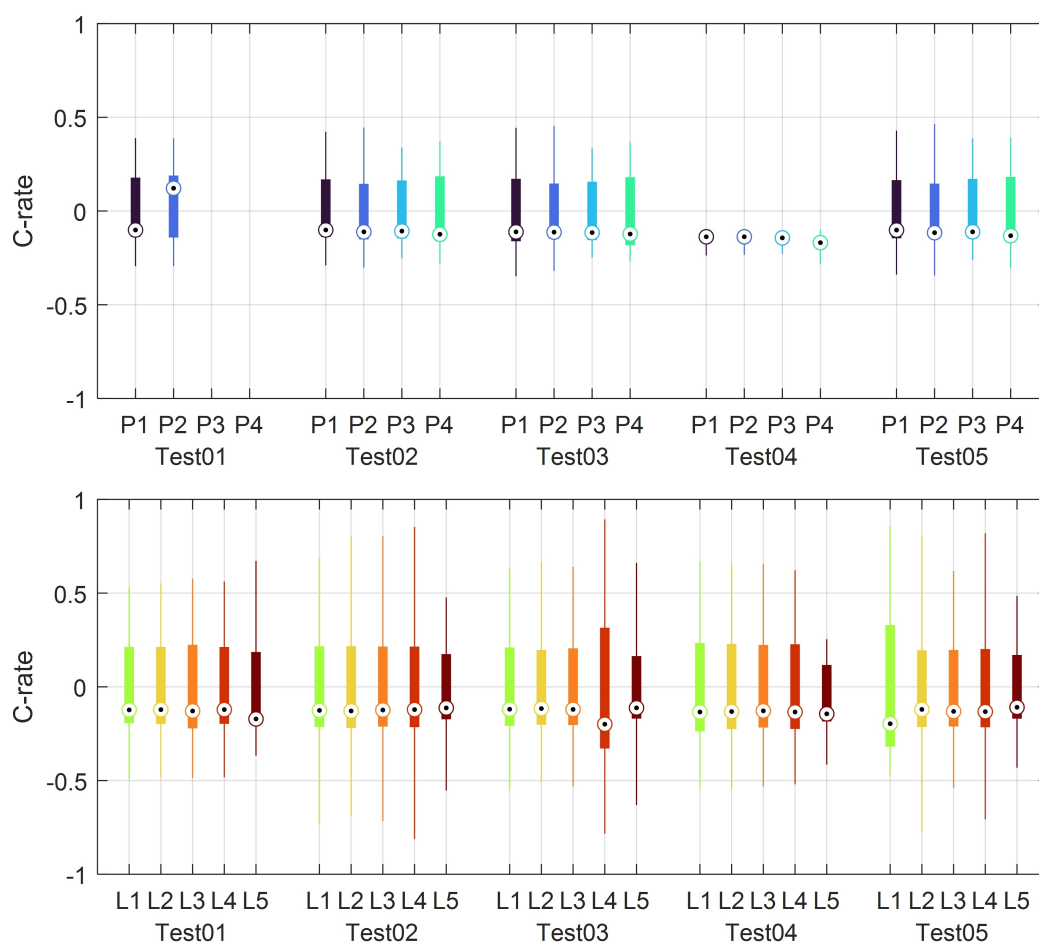
Figure 10. Boxplots of the C-rate distribution for each battery unit of M5BAT. The upper subplot shows the lead-acid batteries while the lower subplot shows the Lithium batteries with the shortened acronyms according to Table 1. Data points with a C-rate of 0 C are not shown here but can be found in Figure A2 in Supporting Information.[35]

the battery units in FCR operation do not have to deliver power. Overall, these are low C-rates, which do not strongly affect cyclic battery aging.

Both investigations demonstrated that level 1 of the SPDA works and the chosen battery units for this level have to deal with higher loads. Level 1 utilizes the battery unit with frequent power requests, which makes the level optimal for cyclic stable batteries.

Energy throughput

The energy throughput, of the battery storage is broken down to the nine active battery units to show the influence the PDAs have. The energy throughput is calculated according to Equation (4). The charged energy E_{cha} is the sum of all power requests P_{ist} lower than 0 kW, while the discharged energy E_{dis} is the sum of all power requests P_{ist} larger than 0 kW. The overall energy throughput E_{ges} is the sum of the absolut value of all power requests P_{ist}.

$$E_{cha} = \sum_{t=0}^{t=end} ((P_{ist}(t) < 0) \cdot t)$$

$$E_{dis} = \sum_{t=0}^{t=end} ((P_{ist}(t) > 0) \cdot t) \qquad (4)$$

$$E_{ges} = \sum_{t=0}^{t=end} (abs(P_{ist}(t)) \cdot t)$$

In Figure 11, no distinction is made between charging and discharging cases, but only the total energy throughput is shown as a percentage and in absolute value. The energy throughput of all battery units is stacked up for each test.

The relative energy throughput in Figure 11 reveals that level 1 of SPDA, which was used in tests 3 and 5, results in the highest energy throughput of the selected battery units (LMO 4 and LMO 1, respectively). It is also clear that the size of the SOC bands in levels 2a and 2b determines what portion of the energy throughput the selected battery units receive. This becomes particularly clear when comparing test 2 with test 4. In test 4, the SOC band of all LMO battery units has been extended downwards by 25%-points. As a result, the shares of the LMO batteries have increased to such an extent that all other battery units are almost no longer used. The less large differences in the SOC bands in test 2 result in a more even use of the battery units. As can be seen in test 1, the dependence on the forecast in level 3 of the power distribution leads to the use of only batteries with good power forecasts. The batteries Pb3 and Pb4 are no longer used here.

The absolute energy value for all battery units combined is shown on top of the bars in Figure 11. The total energy throughput differs between the tests because of the requirements of the FCR. During operation, this can only be influenced additionally to FCR in the form of maintenance charges.

To quantify the equivalent full cycles (EFC) per battery and the cyclic battery aging the nominal energy capacity and nominal number of cycles according to the manufacturer from Table 1 are used. Battery unit LMO 4 fulfilled 28.38 EFC in test 3 compared to 6.5 EFC in test 2. In test 3 the BESS cyclic aging is 6.81‰ while the LMO 4 battery accounts for 4.73‰ of the
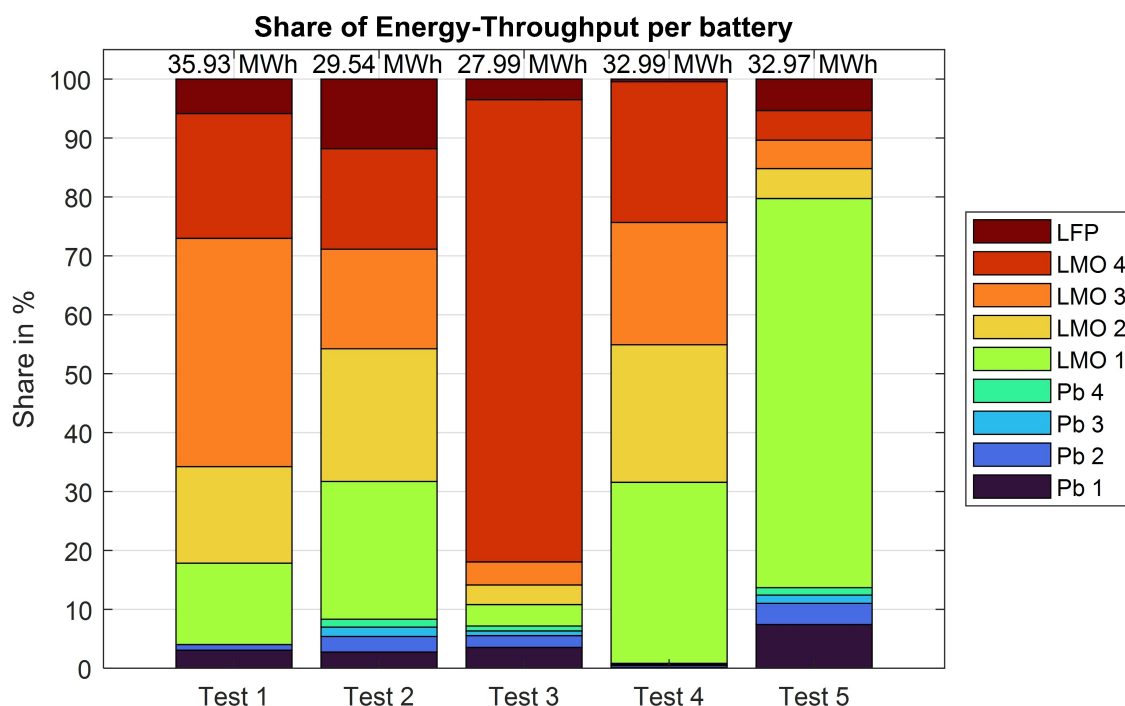

Figure 11. Relative share of energy throughput and absolute energy throughput value for each test.

Batteries & Supercaps

Research Article
doi.org/10.1002/batt.202200414

**Chemistry
Europe**

European Chemical
Societies Publishing

cyclic aging. A symmetrical power distribution would have caused 11.85‰ of cyclic aging to the BESS. In summary, the SPDA stressed the BESS in test 3 with only 57.47% of the cyclic aging compared to a symmetrical power distribution. If a more cyclic stable battery unit like the LTO battery unit was used instead of battery unit LMO 4 the cyclic aging of the BESS could be reduced to 38.74% compared to a symmetrical power distribution.

Efficiency

Since the battery units were used very differently in the tests, the overall efficiencies for each component of the storage system is considered in the efficiency analysis. The efficiency plays a central role in an economic calculation for battery storage, because every increase in efficiency results in lower recharging energy quantities and thus lower costs for setpoint adjustments.

All efficiency values are given as RTE values, which are calculated according to Equation (5). The charging direction for all components is according to Figure 1 from the grid towards the batteries while the discharging direction is defined as an energy flow from the batteries towards the grid.

$$RTE_{BESS} = RTE_{Transformer} \cdot RTE_{Inverter} \cdot RTE_{Battery}$$

$$RTE = \frac{E_{dis}}{E_{cha}} \tag{5}$$

Figure 12 shows the RTE determined for the five tests. The results of the RTE calculations receive a small error, because the states of charge and thus the energy quantities contained at

the beginning and at the end of the test were not identical. To correct this, the SOC difference was converted to an energy difference, which adjusts the energy throughputs to a common start and end SOC. The error bars in Figure 12 show the measurement error, while the calculation of the error bars is described in detail in the appendix. The efficiency analysis shows that the tests with active battery units in prioritization level 1 have a lower overall efficiency. Test 2 with the use of all battery units and setting of SOC bands in levels 2a and 2b shows the best efficiency with just under 75%.

By comparison of only the battery efficiencies between the different tests in Figure 12, test 4 stands out with a higher efficiency. In this test, only the LMO batteries were active for the majority of time. With their higher efficiency, the LMO batteries rise the overall battery efficiency. On the inverter side, test 5 has the highest efficiency value with 91.6%. This suggests that the heavy use of one inverter and the infrequent use of most other inverters, leads to better efficiencies of the inverters.[33,34] On transformer side, the best efficiency with 86.6% was observed in test 2. In this test, the energy throughput is distributed to all battery units and so all individual transformers were used.

Discussion and comparison of power distribution algorithms

Both the status quo PDA and the new SPDA have implemented an inverter threshold power and an inverter hysteresis power which help to minimize low power loads on the inverters and thus increase the efficiency (see section "Large-scale BESS M5BAT" and previous research[16,20,33]). A symmetrical PDA should have implemented this feature as well. In addition, the
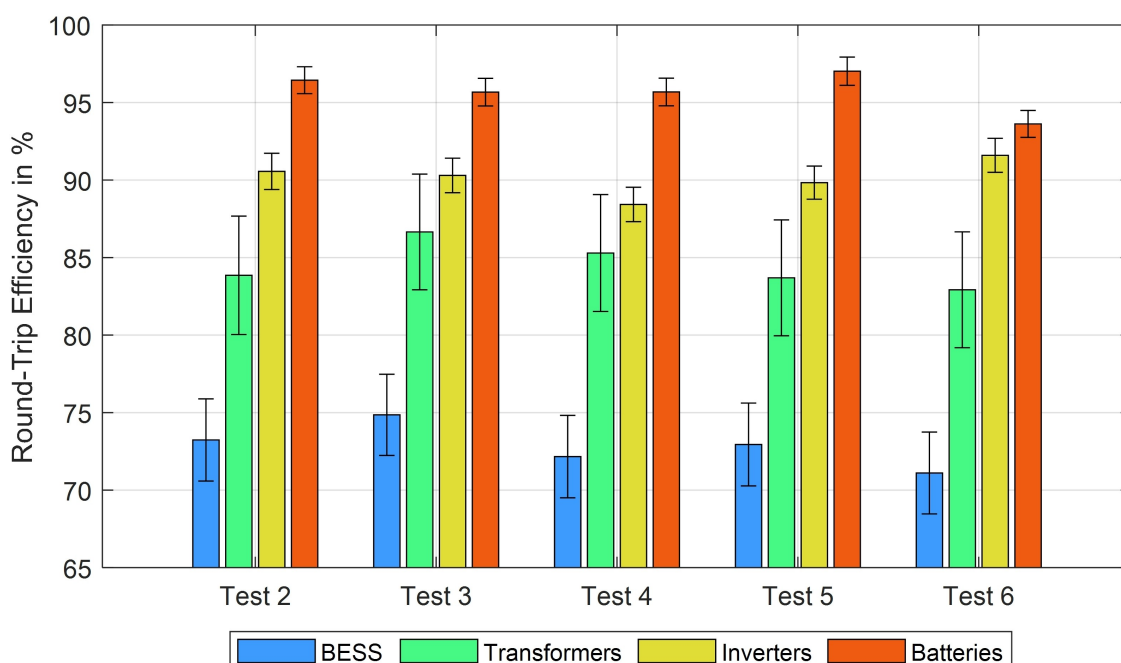

Figure 12. Efficiency for the aggregated components for each test.

Batteries & Supercaps

Research Article
doi.org/10.1002/batt.202200414

Chemistry
Europe
European Chemical
Societies Publishing

described hysteresis should also be present in all PDAs so that load shifting between inverters are kept to a minimum.

As described in section "Status quo power distribution" the status quo PDA favors battery units with a high EPR by sorting the battery units by their power delivery time prognosis. For the large-scale BESS M5BAT, this means that the lead-acid batteries receive a high energy throughput and thus higher cyclic loads. A symmetrical PDA in which the power is distributed proportionally to the battery units' capacity would also favor battery units with a high EPR, similar to the status quo PDA. A symmetrical PDA would keep the battery units at the same SOC levels, which is suboptimal for the calendar aging of the different battery technologies within a hybrid BESS.

In total, this results in earlier end of life for the lead acid batteries (see Table 1) and lowers the total efficiency. With the new SPDA, the energy throughput and thus the cyclic load can be shifted to each battery unit dependent on the user's input parameters (Table 4). Furthermore, the influence on the SOC is clearly visible with regard to the calendar aging of the battery units. It is expected that this will lead to an increase of the lifetime of the individual battery units and improve economics of the whole BESS with the SPDA in comparison to the status quo PDA or a symmetrical PDA.

Moreover, especially battery units with a small EPR like LTO (see Table 1 and Table 3) can profit from the SPDA. They can be used more intense and play out the advantage of cyclic stability and thus improve both economics and longevity of a large-scale hybrid BESS like M5BAT.

Conclusion and Outlook

Power distribution in modular large-scale battery energy storage systems is a core part of the energy management system. It influences the efficiency, the lifetime and thus the overall economics of storage operation. The presented rule-based power distribution algorithm (SPDA) in this paper can target different characteristics of batteries in modular battery energy storage systems. By setting individual SOC bands, the algorithm ensures that these SOC bands are maintained in regular operation. This has the potential to reduce the aging of batteries, while increasing the efficiency of the components. Regarding the calendar aging behavior, the SOC bands can be set individual for each battery to improve the aging technology specific. The cyclic prioritization level, level 1 of the algorithm allows cycle-stable batteries to be used much more frequently than other batteries. Thus, the advantages of a cycle-stable battery can be used specifically in modular or hybrid battery energy storage systems. The shift of nearly 80% of the energy throughput to one battery unit with the SPDA is shown and caused 42.53% less cyclic aging than a symmetrical power distribution algorithm would have caused. Overall, the algorithm has the potential to increase the runtime and lifetime of batteries in this way. Depending on the design, the entire battery energy storage system can become more efficient by using the more efficient battery units more frequently or by

adjusting the hysteresis and workload dependent efficiency of the inverters. Higher efficiencies can be achieved for inverters and transformers.

Further testing and development of the SPDA is possible at improving the BESS efficiency at the transformer side to even higher values. Moreover, the readiness of the algorithm for multi-use purposes should be examined and for FCR with using the DOFs or with a different SPA algorithm investigations are necessary.

Author Contributions

Lucas Koltermann: Conceptualization, Methodology, Software, Validation, Formal Analysis, Investigation, Data Curation, Visualization, Writing - Original Draft

Kevin Jacqué: Conceptualization, Methodology, Software, Validation, Writing - Review & Editing

Jan Figgener: Conceptualization, Validation, Writing - Review & Editing, Supervision

Sebastian Zurmühlen: Validation, Writing - Review & Editing, Project administration, Funding acquisition

Dirk Uwe Sauer: Validation, Resources, Writing - Review & Editing, Supervision, Funding acquisition

Acknowledgements

Conflict of Interest

The authors declare no conflict of interest.

Data Availability Statement

The data that support the findings of this study are available from the corresponding author upon reasonable request.

[1] O. Krishan, S. Suhag, *Int. J. Energy Res.* **2019**, *43*, 6171.
[2] J. Figgener, P. Stenzel, K.-P. Kairies, J. Linßen, D. Haberschusz, O. Wessels, G. Angenendt, M. Robinius, D. Stolten, D. U. Sauer, *J. Energy Storage* **2020**, *29*, 101153.
[3] J. Figgener, P. Stenzel, K.-P. Kairies, J. Linßen, D. Haberschusz, O. Wessels, M. Robinius, D. Stolten, D. U. Sauer, *J. Energy Storage* **2021**, *33*, 101982.
[4] S. Englberger, A. Jossen, H. Hesse, *Cell Rep. Phys. Sci.* **2020**, *1*, 100238.

Batteries & Supercaps

Research Article
doi.org/10.1002/batt.202200414

Chemistry Europe
European Chemical
Societies Publishing

[5] a) M. Dubarry, M. Tun, G. Baure, M. Matsuura, R. E. Rocheleau, *Electronics* **2021**, *10*, 1593; b) P. Eckert, G. Di Lembo, A. Rasic, C. Noce, L. Consiglio, A. Schuette in *22nd International Conference and Exhibition on Electricity Distribution (CIRED 2013)*, Institution of Engineering and Technology, **2013**, p. 781; c) M. Koller, T. Borsche, A. Ulbig, G. Andersson, *Electr. Power Syst. Res.* **2015**, *120*, 128; d) M. Swierczynski, D.-I. Stroe, A.-I. Stan, R. Teodorescu, R. Laerke, P. C. Kjaer in *IEEE PES ISGT Europe 2013*, IEEE, **2013–2013**, pp. 1–5.

[6] F. Karoui, D.-L. Ha, T. Delaplagne, M.-F. Bouaaziz, V. Eudier, M. Lévy, *Energy Procedia* **2018**, *155*, 61.

[7] Luca Lo Schiavo, Michele Benini, 2018 AEIT International Annual Conference (AEIT). Bari (Italy), October 3–5, 2018, IEEE, Piscataway, NJ, **2018**.

[8] J. Figgener, C. Hecht, D. Haberschusz, J. Bors, K. G. Spreuer, K.-P. Kairies, P. Stenzel, D. U. Sauer, *arXiv* **2022**.

[9] The International Renewable Energy Agency (IRENA), *Behind-The-Meter Batteries – Innovation Landscape Brief*, Abu Dhabi, **2019**.

[10] B. Gundogdu, S. Nejad, D. T. Gladwin, D. A. Stone in *Proceedings, 2017 IEEE International Symposium on Industrial Electronics (ISIE). Edinburgh International Conference Centre, Edinburgh, Scotland, United Kingdom, 18–21 June 2017*, IEEE, Piscataway, NJ, **2017**, pp. 26–31.

[11] Commission Regulation (EU) 2017/2195 of 23 November 2017 establishing a guideline on electricity balancing. EB-GL, **2017**.

[12] Deutsche ÜNB, *Prequalification Process for Balancing Service Providers (FCR, aFRR, mFRR) in Germany ("PQ conditions")*, **2020**.

[13] X. Luo, J. Wang, J. Wojcik, J. Wang, D. Li, M. Draganescu, Y. Li, S. Miao, *Energies* **2018**, *11*, 1070.

[14] Deutsche ÜNB, *Eckpunkte und Freiheitsgrade bei Erbringung von Primärregelleistung*, **2014**.

[15] L. Koltermann, K. Jacqué, J. Figgener, S. Zurmühlen, D. U. Sauer, *Int. J. Electr. Power Energy Syst.* **2022**, *142*, 108327.

[16] T. Thien, D. Schweer, D. vom Stein, A. Moser, D. U. Sauer, *J. Energy Storage* **2017**, *13*, 143.

[17] T. Thien, H. Axelsen, M. Merten, D. U. Sauer, *J. Energy Storage* **2022**, *51*, 104257.

[18] J. Münderlein, G. Ipers, M. Steinhoff, S. Zurmühlen, D. U. Sauer, *Int. J. Electr. Power Energy Syst.* **2020**, *119*, 105887.

[19] K. Jacqué, L. Koltermann, J. Figgener, S. Zurmühlen, D. U. Sauer, *Energies* **2022**, *15*, 1342.

[20] Institute for Power Generation and Storage Systems (RWTH Aachen), *Modularer multi-Megawatt multi-Technologie Mittelspannungs-Batteriespeicher (M5BAT). Abschlussbericht, Datenblätter sowie weiteres Aktenarchiv*. Funding code: 03ESP265A, Aachen, **2018**.

[21] J.-Y. Choi, I.-S. Choi, G.-H. Ahn, D.-J. Won, *IEEE Trans. Smart Grid* **2018**, *9*, 1292.

[22] S.-M. Cho, S.-Y. Yun, *Energies* **2017**, *10*, 2092.

[23] M. Mühlbauer, O. Bohlen, M. A. Danzer, *J. Energy Storage* **2020**, *30*, 101415.

[24] M. Muehlbauer, S. Klier, H. Palm, O. Bohlen, M. A. Danzer in *2020 22nd European Conference on Power Electronics and Applications (EPE'20 ECCE Europe)*, IEEE, Piscataway, NJ, **2020**, pp. 1–11.

[25] M. Mühlbauer, F. Rang, H. Palm, O. Bohlen, M. A. Danzer, *J. Energy Storage* **2022**, *48*, 103803.

[26] M. Schimpe, C. Piesch, H. Hesse, J. Paß, S. Ritter, A. Jossen, *Energies* **2018**, *11*, 533.

[27] P. Keil, A. Jossen, *J. Electrochem. Soc.* **2017**, *164*, A6066–A6074.

[28] P. Keil, S. F. Schuster, J. Wilhelm, J. Travi, A. Hauser, R. C. Karl, A. Jossen, *J. Electrochem. Soc.* **2016**, *163*, A1872-A1880.

[29] S. Gantenbein, M. Schönleber, M. Weiss, E. Ivers-Tiffée, *Sustainability* **2019**, *11*, 6697.

[30] M. Ecker, N. Nieto, S. Käbitz, J. Schmalstieg, H. Blanke, A. Warnecke, D. U. Sauer, *J. Power Sources* **2014**, *248*, 839.

[31] J. Schmalstieg, S. Käbitz, M. Ecker, D. U. Sauer, *J. Power Sources* **2014**, *257*, 325.

[32] K. Jacqué, L. Koltermann, J. Figgener, S. Zurmühlen, D. U. Sauer, *J. Energy Storage* **2022**, *52*, 105040.

[33] J. Münderlein, M. Steinhoff, H. Axelsen, D. U. Sauer in *2017 IEEE International Telecommunications Energy Conference (INTELEC)*, IEEE, **2017–2017**, pp. 314–320.

[34] K. Jacqué, L. Koltermann, J. Figgener, S. Zurmühlen, D. U. Sauer, *J. Energy Storage* **2022**, *52*, 104961.

[35] A. Danz, *boxplotGroup*, MATLAB Central File Exchange, **2022**.

[36] L. Koltermann, K. K. Drenker, M. E. Celi Cortés, K. Jacqué, J. Figgener, S. Zurmühlen, D. U. Sauer, *J. Energy Storage* **2023**, *57*, 106190.

[37] DEWETRON elektronische Messgeräte Ges.m.b.H., *DEWE-571 Technical reference manual*, **2009**.

[38] SMA Solar Technology AG, *Sunny Central CP Messwertabweichungen*, **2013**.